Deciphering the Role of Hydrogen Bonding in Enhancing pDNA–Polycation Interactions

ARTICLE *in* LANGMUIR · OCTOBER 2007

Impact Factor: 4.46 · DOI: 10.1021/la7009995 · Source: PubMed

4 AUTHORS, INCLUDING:

Lisa Prevette
University of St. Thomas
10 PUBLICATIONS **387** CITATIONS
SEE PROFILE

Thomas E. Kodger
University of Amsterdam
26 PUBLICATIONS **239** CITATIONS
SEE PROFILE

Deciphering the Role of Hydrogen Bonding in Enhancing pDNA−Polycation Interactions

Lisa E. Prevette,[†] Tom E. Kodger,[‡] Theresa M. Reineke,*[,†] and Matthew L. Lynch[‡]

University of Cincinnati, Department of Chemistry, P. O. Box 210172, Cincinnati, Ohio 45221-0172, and The Procter & Gamble Company, Corporate Research Division, Miami Valley Laboratories, 11810 East Miami River Road, Cincinnati, Ohio 45252-1038

Received April 5, 2007. In Final Form: May 19, 2007

There is considerable interest in the binding and condensation of DNA with polycations to form polyplexes because of their possible application to cellular nucleic acid delivery. This work focuses on studying the binding of plasmid DNA (pDNA) with a series of poly(glycoamidoamine)s (PGAAs) that have previously been shown to deliver pDNA in vitro in an efficient and nontoxic manner. Herein, we examine the PGAA−pDNA binding energetics, binding-linked protonation, and electrostatic contribution to the free energy with isothermal titration calorimetry (ITC). The size and charge of the polyplexes at various ITC injection points were then investigated by light scattering and ζ-potential measurements to provide comprehensive insight into the formation of these polyplexes. An analysis of the calorimetric data revealed a three-step process consisting of two different endothermic contributions followed by the condensation/aggregation of polyplexes. The strength of binding and the point of charge neutralization were found to be dependent upon the hydroxyl stereochemistry of the carbohydrate moiety within each polymer repeat unit. Circular dichroism spectra reveal that the PGAAs induce pDNA secondary structure changes upon binding, which suggest a direct interaction between the polymers and the DNA base pairs. Infrared spectroscopy experiments confirmed both base pair and phosphate group interactions and, more specifically, showed that the stronger-binding PGAAs had more pronounced interactions at both sites. Thus, we conclude that the mechanism of poly(glycoamidoamine)−pDNA binding is most likely a combination of electrostatics and hydrogen bonding in which long-range Coulombic forces initiate the attraction and hydroxyl groups in the carbohydrate comonomer, depending on their stereochemistry, further enhance the association through hydrogen bonding to the DNA base pairs.

Introduction

The transfer of genetic material into cells offers the unique potential for disease- and cell type-specific therapeutics. The success of the many nucleic acid therapeutic strategies is dependent upon the development of delivery vehicles that are capable of nontoxic and efficient cellular drug delivery. Many different approaches to increase DNA transfection have been attempted. For example, viruses have been studied extensively as modalities for nucleic acid transfer because of their natural ability to enter the cell via endocytosis and direct the transport of genetic material into the nucleus.[1] However, immunogenic concerns and the limited DNA loading capacity of viral vectors have encouraged the design of alternative methods of transfection.[2] Non-viral synthetic vectors, such as liposomes, polymers, and dendrimers, have become popular carriers because of their potential to overcome these difficulties.[3] The design of these systems has been focused primarily on improving in vivo stability and cellular uptake. However, effective delivery is also dependent on several additional fundamental parameters that can be optimized in vitro, such as the polycation−DNA binding affinity, the release of intracellular DNA from the endosomes and the vehicle, DNA stability in the cytoplasm, and, for more traditional gene therapy strategies, the targeting of DNA to the nucleus.[4,5]

Polycations are attractive agents for the compaction of DNA; however, their efficacy is often difficult to optimize because high transfection often accompanies high cytotoxicity and vice versa. Cationic polymers effectively bind to negatively charged phosphate groups on the DNA backbone, allowing charge neutralization and compaction.[5−10] The resulting polyplex is recognized by cell surface proteoglycans and has been shown to enter cells via endocytosis.[11−13] Many studies have shown that polymeric vectors can protect DNA from enzymatic degradation that can occur within the cell.[5,11,14] Common polycations, such as polylysine, polyethyleneimine (PEI), and chitosan, have been investigated extensively for this pur-

* Corresponding author. E-mail: theresa.reineke@uc.edu.

[†] University of Cincinnati.

[‡] The Procter & Gamble Company.

(1) (a) Kaneda, Y. *Curr. Mol. Med.* **2001**, *1*, 493−499. (b) Rubanyi, G. M. *Mol. Aspects Med.* **2001**, *22*, 113−142. (c) Smith, A. E. *Annu. Rev. Microbiol.* **1995**, *49*, 807−838.

(2) (a) Verma, I. M.; Somia, N. *Nature* **1997**, *389*, 239−242. (b) Anderson, W. L. *Nature* **1998**, *392*, 25−30. (c) Yla-Herttuala, S.; Martin, J. F. *Lancet* **2000**, *355*, 213−222.

(3) (a) Luo, D.; Saltzman, W. M. *Nat. Biotech.* **2000**, *18*, 893−895. (b) Boussif, O.; Lezoualch, F.; Zanta, M. A.; Mergny, M. D.; Scherman, D.; Demeneix, B.; Behr, J. P. *Proc. Natl. Acad. Sci. U.S.A.* **1995**, *92*, 7297−7301. (c) Ma, H.; Diamond, S. L. *Curr. Pharm. Biotech.* **2001**, *2*, 1−17.

(4) (a) Kostiainen, M. A.; Hardy, J. G.; Smith, D. K. *Angew. Chem., Int. Ed.* **2005**, *44*, 2556−2559. (b) Rungsardthong, U.; Ehtezazi, T.; Bailey, L.; Armes, S. P.; Garnett, M. C.; Stolnik, S. *Biomacromolecules* **2003**, *4*, 683−690. (c) Chen, D. J.; Majors, B. S.; Zelikin, A. N.; Putnam, D. *J. Controlled Release* **2005**, *103*, 273−283.

(5) Liu, Y.; Reineke, T. M. *Bioconjugate Chem.* **2006**, *17*, 101−108.

(6) Davis, M. E.; Pun, S. H.; Bellocq, N. C.; Reineke, T. M.; Popielarski, S. R.; Mishra, S.; Heidel, J. D. *Curr. Med. Chem.* **2004**, *11*, 179−197.

(7) Liu, Y.; Wenning, L.; Lynch, M.; Reineke, T. M. *J. Am. Chem. Soc.* **2004**, *126*, 7422−7423.

(8) Liu, Y.; Reineke, T. M. *J. Am. Chem. Soc.* **2005**, *127*, 3004−3015.

(9) Liu, Y.; Wenning, L.; Lynch, M.; Reineke, T. M. In *Polymeric Drug Delivery: Particulate Drug Carriers*; Svenson, S., Ed.; ACS Symposium Series 923; American Chemical Society: Washington, DC, 2006; Vol. 1, pp 217−227.

(10) Gosule, L. C.; Schellman, J. A. *Nature* **1976**, *259*, 333−335.

(11) Nisha, C. K.; Manorama, S. V.; Ganguli, M.; Maiti, S.; Kizhakkedathu, J. N. *Langmuir* **2004**, *20*, 2386−2396.

(12) Ruponen, M.; Yla-Herttuala, S.; Urtti, A. *Biochim. Biophys. Acta* **1999**, *1415*, 331−341.

(13) Mislick, K. A.; Baldeschwieler, J. D. *Proc. Natl. Acad. Sci. U.S.A.* **1996**, *93*, 12349−12354.

(14) (a) Gao, X.; Huang, L. *Biochemistry* **1996**, *35*, 1027−1036. (b) Abdelhady, H. G.; Allen, S.; Davies, M. C.; Roberts, C. J.; Tendler, S. J. B.; Williams, P. M. *Nucleic Acids Res.* **2003**, *31*, 4001−4005.

10.1021/la7009995 CCC: $37.00
Published on Web 08/18/2007

pose.[13,15−18] There is flexibility in designing polycationic vectors because slight variations in molecular structure (e.g., molecular weight,[19] hydrophobicity,[6] and charge density[7,9]) can have major implications for both transfection and toxicity. For example, PEI is one of the most efficient polymeric vectors because of its high density of amines. Unfortunately, this high amine density is also attributed to a toxic response in most cell lines.[7,20] Chitosan, however, possesses low cytotoxicity but is much less effective at transferring DNA to cells.[21]

Poly(glycoamidoamine)s (PGAAs, Figure 1) previously designed and synthesized in our laboratory have proven to be exceptional gene delivery agents. Studies using these polymeric vectors revealed that they promote high transfection efficiency with minimal toxicity in several cell lines,[5,7−9] and some general trends have emerged with the use of these macromolecule delivery vehicles. When polymers containing the same carbohydrate residue but a different number of secondary amines within the repeat unit were compared, it was found that as the number of amines increased, gene expression increased. Also, the structural characteristics of the polyplexes, the transfection efficiency in certain cell lines, and the dissociation of the polyplexes by an anionic competitor were all affected by the hydroxyl stereochemistry of the carbohydrate (when systems containing the same number of amine residues were compared).[8] Lastly, the polymers within each carbohydrate family that contain four amine groups in the repeat unit were found to produce the highest gene expression.

Such interesting structure−property relationships have inspired this study of the pDNA binding mechanism of the most effective structures. Although there are many hurdles in the transfection process that could be affected by the carbohydrate in the repeat unit (cellular uptake, intracellular trafficking, and toxicity),[22] a better understanding of binding and compaction mechanisms provide insight into many crucial steps during the delivery process. For example, mechanisms involved in forming polyplexes, the ability of these polyplexes to avoid premature dissociation from media counterions and protein competitors, and the eventual release of genetic materials once inside the cell are important parameters to understand. Toward this end, we have employed various biophysical characterization methods, including isothermal titration calorimetry (ITC), ethidium bromide exclusion assay, light scattering, zeta potential, circular dichroism, and FTIR, to further examine PGAA−pDNA binding and the mechanisms involved. We also demonstrate the limitations of commonly used qualititative techniques for measuring DNA binding affinity, such as ethidium bromide exclusion and heparin displacement assays. The results obtained in this study suggest that the binding of PGAAs to pDNA is dependent on both electrostatic and hydrogen bonding interactions, and the differences in these interactions are likely major contributors to the large variation in biological properties observed with these agents.

Table 1. Physical Characteristics of the Poly(glycoamidoamine)s Used for the Studies Herein[a]

polymer	M_w (kDa)	n	M_w/M_n
G4	4.6	11	1.5
D4	4.9	12	1.6
M4	5.9	15	1.3
T4	4.1	12	1.3

[a] Weight-averaged molecular weight (M_w), degree of polymerization (n), and polydispersity index (M_w/M_n).

Materials and Methods

All data are reported as the average of at least three trials using separately prepared polymer and pDNA samples.

Materials. Tris, HEPES, PIPES, sodium citrate, and citric acid were all purchased from Aldrich (Milwaukee, WI). Ethidium bromide (Sigma; St. Louis, MO) and 7.2 kbp pCMV-β DNA (PlasmidFactory; Bielefeld, Germany) were used as received. All buffers (Tris, HEPES, citrate, and PIPES) were made to 10 mM concentration with 18 MΩ purified Millipore water and titrated to the proper pH using HCl or NaOH (Acros; Morris Plain, NJ). Plasmid DNA (pDNA) solution in water was dialyzed extensively against each buffer using Spectra Por 100 molecular weight cutoff membranes (Rancho Dominguez, CA), and the resulting dialysate was used to prepare each polymer solution. DNA concentrations were quantified by absorbance at 260 nm using a molar extinction coefficient of 6600 cm^{-1} M^{-1}.

Poly(glycoamidoamine) Synthesis and Characterization. All PGAAs were prepared and characterized as previously reported.[7−9] Molecular weights (M_w), degrees of polymerization (n), and polydispersity indices (M_w/M_n) are listed in Table 1 for each polymer.

Dynamic Light Scattering and ζ Potential. The charge and size of the polyplexes at different points of formation along the titration curve, corresponding to increasing N/P (polymer secondary amine/DNA phosphate) ratios, were determined at 25 °C using a Zetasizer NanoSeries ZS (Malvern; Worcestershire, U.K.). The instrument employs a 4 mW He−Ne laser operating at 633 nm with a 173° scattering angle. Sample run conditions, including collection time and neutral density attenuation, were automatically assigned. Correlation functions for determining particle size were analyzed by a *z*-average cumulant fit to the data. In the few cases of bimodal correlation functions, the cumulant fit is not adequate (the reported diameter is an average over both distributions); however, it was used here as a general means to show the onset of aggregation. The ζ-potential measurements were collected using the same instrument with laser doppler velocimetry at a 17° scattering angle. Both light scattering and ζ-potential measurements were obtained for 20 μL injections of 5.5 mM polymer solution into 0.31 mM pDNA solution (both in 10 mM Tris buffer, pH 7.4) after thorough mixing of each polymer (**G4**, **D4**, **M4**, **T4**) with pDNA and allowing a 5 min equilibration time before measurement.

Isothermal Titration Calorimetry. Measurements were taken with a VP-ITC (MicroCal, Inc.; North Hampton, MA) at 25 °C. All solutions were formed in 10 mM buffer (either Tris, HEPES, citrate, or PIPES) at pH 7.4 and degassed prior to injection. A 5.5 mM polymer solution was titrated into 1.46 mL of a 0.31 mM pDNA solution using 10 μL injections with a 300 s separation between each injection to allow equilibration. The heat of dilution of the polymer was subtracted by performing a control titration of polymer into buffer. A similar control experiment was performed with the pDNA, and its heat of dilution was found to be negligible. The data were fit to a standard two-site model using Origin 7.0 software, with the enthalpy (ΔH_{obs}), binding constant (K_{obs}), and stoichiometry (n) functioning as free-floating parameters.

The ΔH_{obs} for the binding-linked protonation study were taken as the normalized heat at the second injection of polymer solution into pDNA solution, both in the various 10 mM buffers (Tris, HEPES, PIPES, and citrate) to avoid artifacts contained in the first injection

(15) Davis, M. E. *Curr. Opin. Biotechnol*. **2002**, *13*, 128−131.
(16) Han, S.; Mahato, R. I.; Sung, Y. K.; Kim, S. W. *Mol. Ther*. **2000**, *2*, 302−317.
(17) De Smedt, S. C.; Demeester, J.; Hennink, W. E. *Pharm. Res*. **2000**, *17*, 113−126.
(18) Pannier, A. K.; Shea, L. D. *Mol. Ther*. **2004**, *10*, 19−26.
(19) Godbey, W. T.; Wu, K. K.; Mikos, A. G. *J. Biomed. Mater. Res*. **1999**, *45*, 268−275.
(20) (a) Fischer, D.; Bieber, T.; Li, Y.; Elsasser, H. P.; Kissel, T. *Pharm. Res*. **1999**, *16*, 1273−1279. (b) Chollet, P.; Favrot, M. C.; Hurbin, A.; Coll, J.-L. *J. Gene Med*. **2002**, *4*, 84−91. (c) Godbey, W. T.; Mikos, A. G. *J. Controlled Release* **2001**, *72*, 115−125.
(21) MacLaughlin, F. C.; Mumper, R. J.; Wang, J.; Tagliaferri, J. M.; Gill, I.; Hinchcliffe, M.; Rolland, A. P. *J. Controlled Release* **1998**, *56*, 259−272.
(22) (a) Grosse, S.; Aron, Y.; Honore, I.; Thevenot, G.; Danel, C.; Roche, A.-C.; Monsigny, M.; Fajac, I. *J. Gene Med*. **2004**, *6*, 345−356. (b) Grosse, S.; Tremeau-Bravard, A.; Aron, Y.; Briand, P.; Fajac, I. *Gene Ther*. **2002**, *9*, 1000−1007. (c) Monsigny, M.; Rondanino, C.; Duverger, E.; Fajac, I.; Roche, A.-C. *Biochim. Biophys. Acta* **2004**, *1673*, 94−103.

due to the long equilibration time and possible syringe leakage. The titration conditions were the same as those given above.

To determine the electrostatic contribution to the free energy of binding, we titrated 5.5 mM **G4** or **D4** into 0.31 mM pDNA in 10 mM Tris buffer at pH 7.4. The titration conditions were also the same as those given above, with the addition of 15−300 mM NaCl to the buffer before the solutions were prepared. The data were fit to a standard two-site model using Origin 7.0 software, as described above.

Circular Dichroism. All spectra were obtained using a Jasco J-715 spectropolarimeter (Easton, MD) and 0.1 cm path length cuvette at 25 °C. A 0.31 mM pDNA solution in 10 mM Tris buffer at pH 7.4 was titrated with a 5.5 mM polymer solution in the same buffer by stepwise addition. A 5 min equilibration time was allowed to study conformation changes of DNA at different N/P ratios. Spectra were measured as an average of three scans from 200 to 350 nm at a scan rate of 50 nm/min with a resolution of 0.5 nm.

Fourier Transform Infrared Spectroscopy. All spectra were recorded on a Perkin-Elmer Spectrum One instrument (Wellesley, MA) using attenuated total reflectance with a 45° ZnSe crystal of effective path length 12 μm at 25 °C. Spectra were obtained from 900 to 4000 cm^{-1} at 4 cm^{-1} resolution by accumulating 200 interferograms. Subtraction of the solvent (10 mM Tris buffer) was performed using the water combination mode at 2200 cm^{-1} as a reference.[23] Seven-point Satvisky−Golay smoothing was included, and peak positions were assigned with Omnic software. The pDNA concentration used here was kept constant at 12 mM, and various volumes of 27 mM **G4**, **D4**, **M4**, or **T4** were added to form polyplexes of the desired N/P ratios of 0.25, 0.75, 1.3, and 2.5, respectively.

Ethidium Bromide Exclusion Assay. The fluorescence of ethidium bromide (EB) upon intercalation with DNA (and subsequent decrease upon EB exclusion via PGAA binding) was used to compare the relative pDNA binding affinities of the polymers, according to the method of Read et al.[24] Fluorescence measurements were acquired using a Varian Cary spectrofluorometer with $\lambda_{ex} = 510$ nm, $\lambda_{em} =$ 590 nm, a 10 nm slit width, and an integration time of 3 s. All solutions were made in 10 mM Tris buffer at pH 7.4. The fluorescence of a 400 ng/mL EB solution (F_{bg}) and that of a 10 μg/mL solution of pDNA containing 400 ng/mL EB (F_{DNA}) were first measured as controls. EB exclusion assays were completed with each polymer and pDNA by titrating 2.0 mL of the F_{DNA} solution with aliquots (50 μL of a 26 μg/mL polymer solution) of each polymer corresponding to 0.5 N/P ratio (moles of polymer secondary amines/moles of pDNA phosphates). After the addition of each 50 μL polymer aliquot, the solution was gently mixed, and the reduced fluorescence (F_x) was measured. The % relative fluorescence (%F) was determined using the equation below:

$$\%F = 100 \times \frac{F_x - F_{bg}}{F_{DNA} - F_{bg}}$$

Results

Particle Size and Zeta Potential. The hydrodynamic diameter of the polyplexes at various stages of formation, between N/P = 0 and 4.5, was studied by dynamic light scattering (Figure 2). Data for the free plasmid (N/P = 0) was not included because of the inaccuracy of fitting the correlation function with the equation based on spherical particles. (The tertiary structure of pDNA involves mostly plectonemic supercoiling,[25] which gives the plasmid a rodlike shape in solution.) The polyplexes were relatively stable in size between 184 and 238 nm as the N/P was further increased between 0.25 and about 2.5 for all polymers.

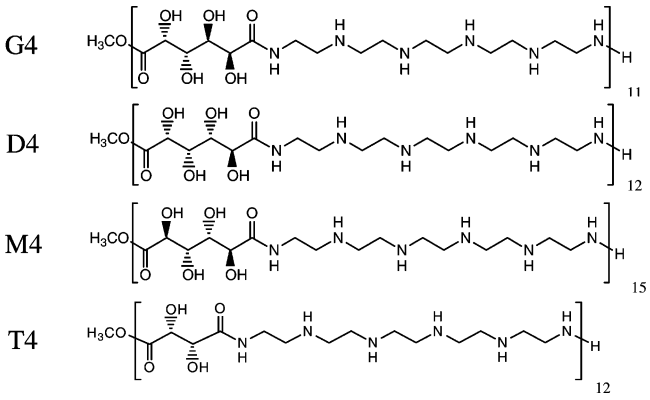

Figure 1. Schematic structures of the four previously synthesized poly(glycoamidoamine)s that contain four secondary amines and a carbohydrate unit, either *meso*-galactaramide (**G4**), D-glucaramide (**D4**), D-mannaramide (**M4**), or L-tartaramide (**T4**), within the repeat unit.[7−9]

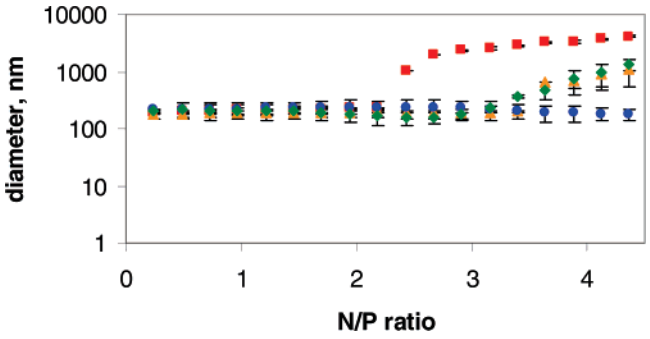

Figure 2. Particle size of polyplexes formed during the titration of a 0.31 mM solution of pDNA in 10 mM Tris buffer (pH 7.4) with a 5.5 mM solution of (■) **G4**, (◆) **T4**, (▲) **D4**, and (●) **M4** dissolved in the same buffer.

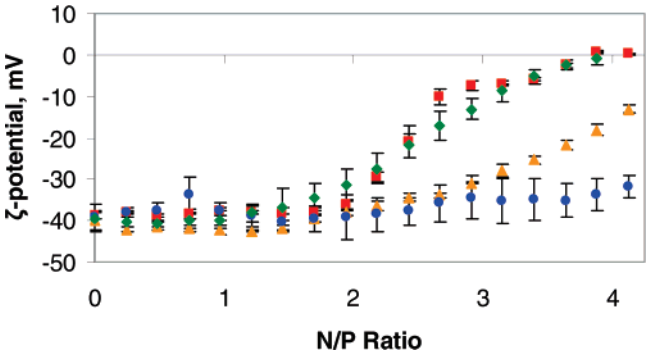

Figure 3. Zeta potential of polyplexes formed during the titration of a 0.31 mM solution of pDNA in 10 mM Tris buffer (pH 7.4) with a 5.5 mM solution of (■) **G4**, (◆) **T4**, (▲) **D4**, and (●) **M4** dissolved in the same buffer.

After this point, a large increase in polyplex diameter to micrometer-scale particles was observed for **G4**, representing the aggregation of polyplexes due to van der Waals forces and reduced charge repulsion. The same effect was seen at N/P = 3.5 for **T4** and **D4** polyplexes, but flocculation was not seen in polyplexes formed with **M4** over N/P from 0.25 to 4.5.

Because interparticle attraction and thus aggregation are expected when enough phosphate neutralization has occurred on the pDNA to prevent charge repulsion (considered to occur at approximately ±20−30 mV), particle size data should correlate well with the ζ-potential measurements. As shown in Figure 3, polyplexes prepared using **G4** or **T4** reached charge neutrality at a similar N/P ratio of 3.8. **D4** was less effective at neutralizing

(23) Alex, S.; Dupuis, P. *Inorg. Chim. Acta* **1989**, *157*, 271−281.
(24) Read, M. L; Bettinger, T.; Oupicky, D. In *Nonviral Vectors for Gene Therapy*; Findeis, M. A., Ed.; Methods in Molecular Medicine; Humana Press: Totowa, NJ, 2001; Vol. 65, pp 131−148.
(25) (a) Boles, T. C.; White, J. H.; Cozzarelli, N. R. *J. Mol. Biol.* **1990**, *213*, 931−951. (b) Lyubchenko, Y. L.; Shlyakhtenko, L. S. *Proc. Natl. Acad. Sci. U.S.A.* **1997**, *94*, 496−501.

the pDNA phosphate charges upon binding, as evidenced by the higher amount of polymer necessary to observe a decrease in the negative surface charge of **D4** polyplexes. The inability of **M4** to significantly affect the surface charge of its polyplexes in this N/P range suggested a weaker interaction with pDNA. It is interesting that the trend that emerged through ζ-potential did not coincide exactly with the point of polyplex aggregation in the case of **T4**, for which −20 mV was reached at N/P of about 2.5, but flocculation did not occur until approximately N/P = 3.5. This discrepancy is attributed to the heterogeneity of the polymer samples. These morphological results reveal that the point of compaction, charge neutrality, and thus aggregation differ for polyplexes formed with the four poly(glycoamidoamine)s.

Thermodynamics of Binding. Isothermal titration calorimetry was used to compare the polymer binding strength and the role of the hydroxyl number and stereochemistry in the thermodynamic parameters. Heat change as a result of the interaction was measured at each injection of polymer, and this information was fit to an equation by nonlinear least-squares analysis to calculate the association constant, enthalpy, and entropy.[26]

The extreme sensitivity of this technique results in a summation of heat effects determining the shape of the isotherm. To obtain accurate thermodynamic binding parameters, the nonbinding heat contributions must be subtracted before applying the curve-fitting algorithms. These extraneous contributions include those from the dilution of both polymer and DNA solutions, aggregation of the resultant polyplexes, coupled protonation effects, and possible conformation changes upon binding.

Three consecutive processes were observed in the thermograms for all of the poly(glycoamidoamine)s binding to pDNA after the subtraction of polymer dilution heats, as indicated by the different slopes in the isotherms (Figure 4). The existence of a bimodal isotherm for the interaction between multivalent cations and both linear and plasmid DNA has previously been observed[27,28] and analyzed by the complexation−condensation model developed by Ehtezazi et al.[28] This model is based on the assumption that binding density increases with polymer concentration, and that when the number of neutralized charges on DNA reaches a critical value, DNA condenses and precipitates.[29] Applying similar reasoning to our coupled light scattering and zeta potential data, the third region of the **G4**, **T4**, and **D4** thermograms (after the second slope) contains the heat of condensation/aggregation. (Previous studies have shown that distinguishing between condensation and aggregation is hindered by the association of several molecules into an insoluble complex that phase separates from solution.[30]) Thus, to fit the data to a model based solely on binding, points possessing such heat contributions were subtracted from the final isotherms, which has been done previously by Patel and Anchordoquy for lipospermine−pDNA binding studies.[27]

According to the particle size data in Figure 2, initial heat effects signal only the binding of polymers to pDNA and contain no condensation/aggregation contribution until an N/P ratio of 2.2 or greater is reached, depending upon the structure of the carbohydrate co-monomer. Therefore, standard two-site model

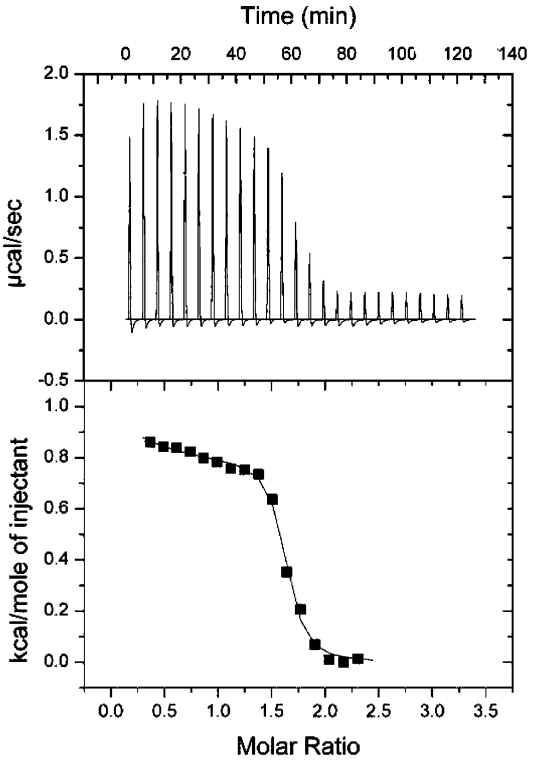

Figure 4. Isothermal titration calorimetry (ITC) thermogram for 5.5 mM **T4** titrated into 0.31 mM pDNA showing two types of binding and small heats of aggregation. Here, site 1 was defined as those points between molar ratios 0 and 1.3, site 2 as those between 1.3 and 2.0, and the point of aggregation was assigned to all points above a molar ratio of 2.3. Points containing aggregation heats (as determined via light scattering) were subtracted from the final figure before performing the curve-fitting routine.

Table 2. Thermodynamic Parameters of the Binding Interaction between the PGAAs and pDNA − Site 1

polymer	$K_1 \times 10^{-5}$, M^{-1}	n_1	ΔH_1, kcal/mol	ΔS_1, kcal/mol·K
G4	9.23 ± 0.15	1.39 ± 0.00	0.628 ± 0.009	0.0260 ± 0.0001
D4	108 ± 23	0.823 ± 0.179	0.856 ± 0.248	0.0358 ± 0.0013
M4	10.6 ± 11.3	0.219 ± 0.043	0.485 ± 0.099	0.0256 ± 0.0028
T4	17.1 ± 10.4	0.935 ± 0.658	0.885 ± 0.196	0.0311 ± 0.0020

Table 3. Thermodynamic Parameters of the Binding Interaction between the PGAAs and pDNA − Site 2

polymer	$K_2 \times 10^{-5}$, M^{-1}	n_2	ΔH_2, kcal/mol	ΔS_2, kcal/mol·K
G4	158 ± 26	0.425 ± 0.001	0.468 ± 0.004	0.0345 ± 0.0003
D4	5.97 ± 1.64	1.11 ± 0.31	0.737 ± 0.077	0.0287 ± 0.0012
M4	0.135 ± 0.076	1.44 ± 0.79	0.362 ± 0.074	0.0193 ± 0.0012
T4	13.8 ± 2.6	0.629 ± 0.162	1.01 ± 0.38	0.0345 ± 0.0067

fitting procedures were performed on the region of the experimental isotherm prior to aggregation to obtain the Gibbs free energy, enthalpy, entropy, a binding constant, and the stoichiometry of the interaction (Tables 2 and 3). The two-site model employs the following fitting equation that incorporates Langmuir isotherm binding equilibria for two independent types of association, where Q is the heat per injection, M is the macromolecule concentration, V is the volume of the cell, n and ΔH are the stoichiometry and enthalpy of the interactions, respectively, and Θ is the fraction of ligand bound to the macromolecule:

$$Q = MV(n_1\Theta_1\Delta H_1 + n_2\Theta_2\Delta H_2)$$

(26) Wiseman, T.; Williston, S.; Brandts, J. F.; Lin, L.-N. *Anal. Biochem.* **1989**, *179*, 131−137.
(27) Patel, M. M.; Anchordoquy, T. J. *Biophys. J.* **2005**, *88*, 2089−2103.
(28) Ehtezazi, T.; Rungsardthong, U.; Stolnik, S. *Langmuir* **2003**, *19*, 9387−9394.
(29) (a) Porschke, D. *Biochemistry* **1984**, *23*, 4821−4128. (b) Rau, D. C.; Parsegian, V. A. *Biophys. J.* **1992**, *61*, 260−271.
(30) (a) Bloomfield, V. A. *Biopolymers* **1997**, *44*, 269−282. (b) Kabanov, V. A. *Macromolecular Complexes in Chemistry and Biology*; Dubin, P., Ed.; Spring-Verlag: Berlin, 1994; pp 151−174.

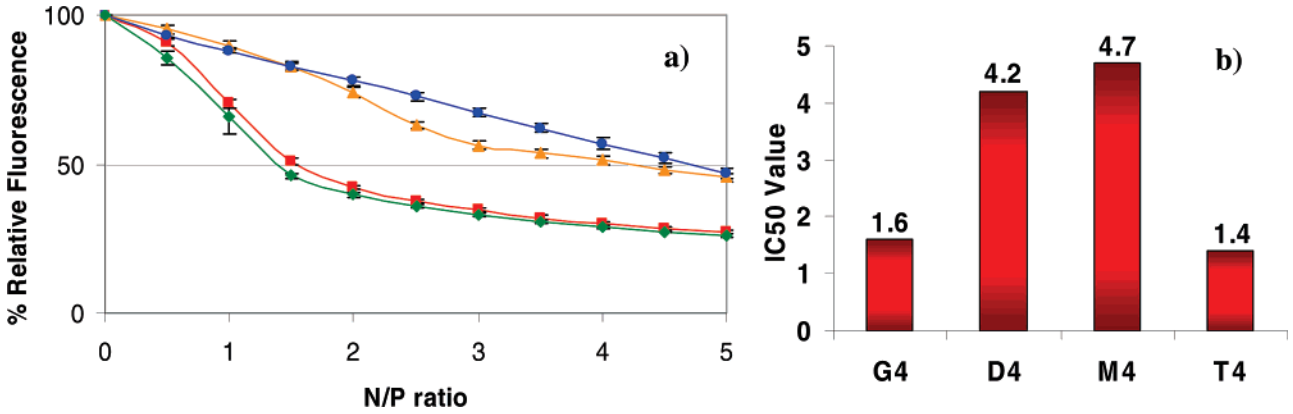

Figure 5. (a) Ethidium bromide exclusion assay results of 10 μg/mL pDNA in 10 mM Tris buffer at pH 7.4 with 26 μg/mL (■) **G4**, (◆) **T4**, (▲) **D4**, and (●) **M4**. (b) Inhibitory concentration (IC_{50}) values, represented as N/P ratios, for poly(glycoamidoamine)s as determined by the ethidium bromide exclusion assay.

One can solve for Θ using the equilibria equations for binding constants K_1 and K_2, with X as the concentration of ligand and [X] as the concentration of free ligand.

$$K_1 = \frac{\Theta_1}{(1-\Theta_1)[\mathrm{X}]} \text{ and } K_2 = \frac{\Theta_2}{(1-\Theta_2)[\mathrm{X}]}$$

$$[\mathrm{X}] = \mathrm{X} - M(n_1\Theta_1 + n_2\Theta_2)$$

To achieve an accurate fit of all six floating variables to our data, multiple attempts were performed starting from different initial parameters. The same six values were reached at the minimum χ^2, regardless of the values of initialization.

The pDNA binding constants obtained for the poly(glycoamidoamine)s are on the order of 10^4-10^7 M^{-1} (Tables 2 and 3), which is in agreement with previously reported values for other cationic polymers[27,31] and for the interaction between many proteins and DNA.[32] Enthalpy is a combination of electrostatics, protonation events, and hydrogen bonding interactions; therefore, ΔH could not be strictly related to any one contribution. However, the binding reaction is slightly endothermic in Tris buffer and thus entropically driven, as seen in many electrostatic associations by the release of counterions and solvent upon attraction of the two polyelectrolytes.[27,31,33]

Entropy values were more consistent, especially those pertaining to site 1. Because all of the structures have the same amine number within the repeat unit, the charge interaction *should* theoretically be analogous among **G4**, **T4**, **D4**, and **M4**. If so, then we should observe a similar release of counterions and solvent upon binding and thus similar entropy contributions and binding constants, which were observed with **G4**, **M4**, and **T4** for site 1. However, the increased K_1 and ΔS_1 values for **D4**−pDNA binding are not currently understood, and more experiments need to be performed to explain this anomaly.

Ethidium Bromide Exclusion Assay. Ethidium bromide (EB) is a well-known DNA intercalator that exhibits an increase in fluorescence intensity upon DNA intercalation. The ability of a competitor, such as a polycation, to reduce this fluorescence by EB exclusion is indicative of its DNA binding strength, which is reported by the IC_{50} value (the N/P ratio of polymer necessary to inhibit 50% of the relative EB−DNA fluorescence). Results for the four glycopolymers, in Figure 5, show that **G4** and **T4** appeared to interact more strongly with pDNA, possessing IC_{50} values of 1.6 and 1.4, respectively. **D4** and **M4** binding affected ethidium bromide exclusion to a lesser extent, as shown by the decidedly smaller slopes in the relative fluorescence upon increasing the N/P ratio. It must be noted that because of the nature of this study, only the relative binding affinities of the PGAAs to pDNA (**T4** ≥ **G4** > **D4** > **M4**) can be determined. The relative strength of binding between **G4**, **D4**, **M4**, and **T4** determined by EB exclusion further supports the role that hydroxyl stereochemistry plays in the association of pDNA with four otherwise very similar polycations.

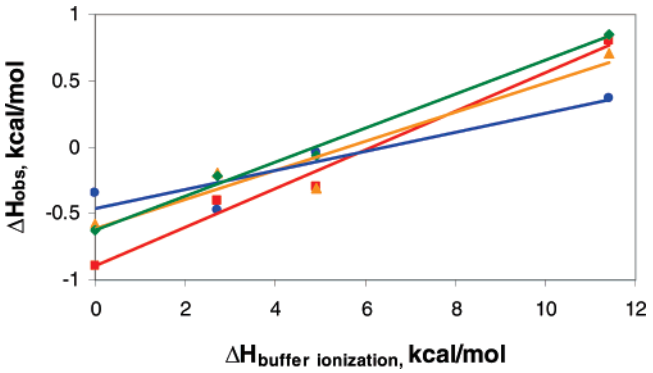

Figure 6. Observed enthalpy of reaction of 5.5 mM (■) **G4**, (◆) **T4**, (▲) **D4**, and (●) **M4** titrated into 0.31 mM pDNA in 10 mM pH 7.4 buffers of varying ionization enthalpy: citrate (0.0 kcal/mol), PIPES (2.7 kcal/mol), HEPES (4.9 kcal/mol), and Tris (11.4 kcal/mol).

PGAA Protonation Upon Binding. To determine the buffer effect on binding energetics and to screen out the contribution of coupled protonation effects, the observed enthalpy of binding between the PGAAs and pDNA in varying buffers of constant pH and ionic strength was plotted versus the buffer ionization enthalpy (Figure 6). As previously shown by Baker and Murphy, the linearity of the results indicates the uptake of protons upon binding.[34] The neutralization of the cationic amine charge by pDNA phosphate groups enables the increase in pK_a of other ionizable secondary amines in the polymer. The number of protons taken up by the polymer upon binding is given by the slope of the fit to the following linear equation, where ΔH_o is the buffer-independent binding enthalpy:[34]

(31) (a) Nisha, C. K.; Manorama, S. V.; Ganguli, M.; Maiti, S.; Kizhakkedathu, J. N. *Langmuir* **2004**, *20*, 2386−2396. (b) Zhou, Y.-L.; Li, Y. Z. *Spectrochim. Acta, Part A* **2004**, *60*, 377−384.

(32) (a) Milev, S.; Bosshard, H. R.; Jelesarov, I. *Biochemistry* **2005**, *44*, 285−293. (b) Engler, L. E.; Welch, K. K.; Jen-Jacobson, L. *J. Mol. Biol*. **1997**, *269*, 82−101.

(33) (a) Manning, G. S. *J. Chem. Phys*. **1969**, *51*, 924−933. (b) Manning, G. S. *Q. Rev. Biophys*. **1978**, *11*, 179−246.

(34) Baker, B. M.; Murphy, K. P. *Biophys. J.* **1996**, *71*, 2049−2055.

$$\Delta H_{obs} = n\Delta H_{ioniz} + \Delta H_o$$

According to this study, **G4** has an intrinsic binding enthalpy of −0.89 kcal/mol, which is slightly less than that reported for PEI (−1.2 kcal/mol) by Choosakoonkriang et al.[35] From the plot of ΔH_{obs} versus ΔH_{ioniz}, the magnitude of ΔH_o (y intercept) decreases according to **G4** > **T4** = **D4** > **M4** (Figure 6, Table 4), which indicates the heat released upon binding. A less negative value (less exothermic) could be due to the formation of fewer hydrogen bonds in **T4**, **D4**, and **M4** polyplexes owing to their hydroxyl stereochemistry. The interaction of these poly(glycoamidoamine)s with pDNA, after eliminating buffer ionization heats, is mildly exothermic. This small enthalpy of binding is evidence of entropy being the driving force behind the interaction. During the association at physiological pH, 0.072−0.15 moles of protons per mole of secondary amine are taken up by the polymers, depending on their binding strength (as determined from the slopes in Figure 6).[34] For example, because **M4** has a weaker interaction with pDNA than **D4**, fewer **M4** secondary amines experience a pK_a shift upon binding, resulting in fewer protons being taken up by this polymer than by **D4**.

Electrostatic Contribution to the Free Energy of Binding. Salt-dependent effects are known to play a role in intermolecular polyion association. They usually arise in the electrostatic component of the interaction because of either charge shielding or competitive ion binding[36] and in the case of nucleic acids are often described in terms of Manning's counterion condensation (CC) theory.[31] This theory treats DNA as a linear array of point charges characterized by its charge density parameter, $\xi = e^2/\epsilon kTb$, where ϵ is the dielectric constant of the bulk solvent, kT is the thermal energy, e is the charge on an electron, and b is the axial spacing between DNA charge groups (0.17 nm for B-DNA). Manning assigns counterions to one of two distinct populations: "condensed" ions are bound within a certain volume around the helix, and "free" ions are described by Debye−Huckel theory. Record et al. extended CC theory to ligand−DNA interactions by determining a linear relationship between the observed binding constant and the concentration of added salt.[35] By manipulating the counterion concentration present during binding, the electrostatic contribution to the free energy, ΔG^o_{es}, can be determined. The association constant of an electrostatic interaction, and thus the total ΔG^o_{obs}, decreases as the concentration of NaCl increases, according to:[33,37]

$$\Delta G^o_{obs} = -RT \ln K_{obs}$$

$$\Delta G^o_{es} = -aRT \ln [M^+]$$

$$\Delta G^o_{ns} = \Delta G^o_{obs} - \Delta G^o_{es}$$

where

$$a = \frac{\partial \ln K_{obs}}{\partial \ln [M^+]}$$

K_{obs} is the binding constant at a particular concentration of NaCl, $[M^+]$, and ΔG^o_{ns} is the nonelectrostatic contribution to the free energy. In this case, the temperature (T) was 298 K, and $[M^+]$ ranged from 15 to 300 mM. We chose to study the effect of competing salt for both **G4** and **D4** interactions with pDNA because **D4** possesses the highest K_1 value and **G4** possesses the lowest.

Table 4. Intrinsic pDNA Binding Enthalpy, ΔH_o, and Moles of Protons per Mole of Secondary Amine, n, Taken Up by the Four PGAAs upon pDNA Binding[a]

	n	ΔH_o, kcal/mol	R^2
G4	0.15	−0.89	0.98
T4	0.13	−0.62	0.99
D4	0.11	−0.62	0.92
M4	0.072	−0.46	0.86

[a] Values Are determined from the slope (n) and y intercept (ΔH_o) of the linear fit of ΔH_{obs} versus $\Delta H_{buffer\ ionization}$ for each polymer. The R^2 value for the linear fit is also provided.

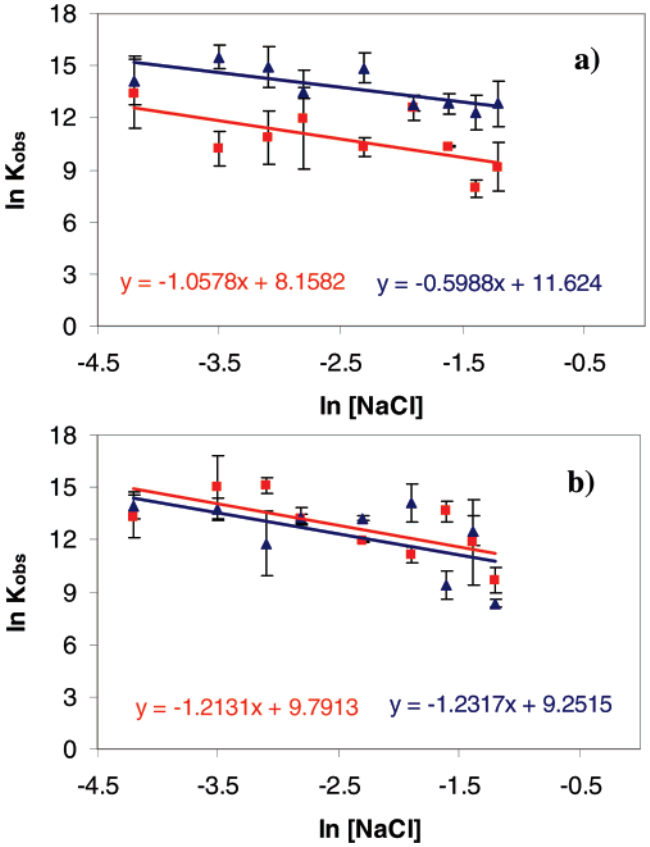

Figure 7. Variation of (■) K_1 and (▲) K_2 upon pDNA complexation with (a) **G4** and (b) **D4** in 10 mM Tris buffer (pH 7.4) at [NaCl] between 15 and 300 mM, as measured by ITC after fitting the isotherm with the two-site binding model. A plot of ln K_{obs} versus ln [NaCl] yields the slope, a, used to calculate ΔG°_{es}.

As shown in Figure 7, adding NaCl to the Tris buffer used in the polymer and pDNA solutions for our ITC experiments produced the expected shielding effect of decreasing K with increasing monovalent ions for both **G4** and **D4**. However, the extent of the salt effect on the interactions of each polymer with pDNA varied. In the case of **D4** (Figure 7b), the value of a (the slope of the lines shown in Figure 7) was −1.2 for both K_1 and K_2, demonstrating the equal electrostatic component to the free energy present in both sites of **D4**−pDNA complexation. Added NaCl reduced the affinity of sites 1 and 2 differently for the **G4** polymer. As shown in Figure 7a, a was −1.1 for K_1 and −0.60 for K_2. Table 5 provides the calculated free energy contributions from two experiments with different added salt concentrations (15 and 300 mM NaCl). In the case of both sites for both polymers, the nonelectrostatic force is the dominant contribution, as demonstrated by the larger magnitudes of the ΔG°_{ns} values. This

(35) Choosakoonkriang, S.; Lobo, B. A.; Koe, G. S.; Koe, J. G.; Middaugh, C. R. *J. Pharm. Sci.* **2003**, *92*, 1710−1722.
(36) Murphy, K. P.; Waldron, T. T.; Schrift, G. L. In *Biocalorimetry 2*. Ladbury, J. E., Doyle, M. L., Eds.; John Wiley & Sons: West Sussex, U.K., 2004; pp 93−104.
(37) Record, M. T.; Anderson, C. F.; Lohman, T. M. *Q. Rev. Biophys.* **1978**, *11*, 103−178.

Table 5. Contributions to the Free Energy of G4− and D4−pDNA Binding as Determined in (a) 15 mM and (b) 300 mM NaCl in 10 mM Tris Buffer, pH 7.4, at 25 °C[a]

		(a)		(b)	
		G4	**D4**	**G4**	**D4**
site 1	$\Delta G°_{obs}$	−7.93	−7.90	−5.43	−5.72
	$\Delta G°_{es}$	−2.74	−2.98	−0.782	−0.853
	$\Delta G°_{ns}$	−5.19	−4.92	−4.65	−4.87
site 2	$\Delta G°_{obs}$	−8.36	−8.25	−7.58	−4.93
	$\Delta G°_{es}$	−1.49	−2.98	−0.426	−0.853
	$\Delta G°_{ns}$	−6.87	−5.27	−7.15	−4.08

[a] $\Delta G°_{es}$ is the electrostatic contribution, and $\Delta G°_{ns}$ is the nonelectrostatic contribution. All energy values are in kcal/mol.

result was unanticipated on the basis of the neutralization of the ζ-potential upon increasing N/P ratio (Figure 3), which certainly provides evidence of electrostatic binding, and the entropic driving force for both sites (Tables 2 and 3).

pDNA Conformation Changes. The extent of polycation-induced pDNA conformation change was investigated by circular dichroism to further characterize the interactions exhibited by the four poly(glycoamidoamine)s. There is no absorbance from the PGAAs above 230 nm, so the spectra exhibit pDNA molar ellipticity only. As demonstrated in Figure 8, pDNA in its native form has a B conformation in the CD spectrum, consisting of both a positive and a negative Cotton effect at 274 and 246 nm, respectively.[38,39] The binding of all PGAAs induced a consistent change in the pDNA secondary structure, causing what was once thought to be a B→C change.[40] This conclusion was substantiated by the red shift in the spectra and the loss of rotational strength of the positive band upon addition of polymer from 0 to 10 N/P ratio. Such CD spectral changes can be attributed to the number of base pairs per helix turn decreasing from 9.3 to 10, an increase in the base angle in relation to the helix axis, and the base pairs slightly separating.[40] The strongest binders, **G4** and **T4**, had the greatest effect on the conformation of the pDNA, with a total loss of positive ellipticity at N/P = 1.5 for **G4** and 3.0 for **T4**. On the basis of these observations, pDNA base pair spacing and tilt are influenced more by **G4** and **T4** than the other two PGAAs, and the weakest pDNA binder, **M4**, has no significant secondary structure effect upon pDNA until N/P = 1.5.

pDNA Binding Sites. The infrared spectral features of PGAA−pDNA polyplexes at various N/P ratios were identified to shed some light on the specific regions of binding between the two macromolecules. There are several regions of interest in the 900−2000 cm^{-1} window for the nucleic acid solution as well as that of the polyplex. The two strong absorptions located at 1222 and 1088 cm^{-1} are attributed to the asymmetric and symmetric phosphate stretches, respectively.[42] As shown in Figure 9 and in the Supporting Information, great intensity increases for the PGAAs were witnessed at these two wavenumbers. The region of 1450−1750 cm^{-1} corresponds to in-plane vibrations of the nucleotide bases, in particular, the guanine carbonyl (1717), thymine carbonyl (1663), adenine C═N (1609), and guanine imidazole nitrogen (1492) stretches.[42] Inevitable water vapor present in the system can provide O−H bending bands between 1600 and 1700 cm^{-1}, partially obscuring this region (variation in background water vapor occasionally resulted in negative spectral characteristics). Also, the polymer amides absorb around 1630 cm^{-1}, which complicated the analysis of both the thymine and adenine interactions; therefore, we have chosen to focus on both guanine vibrations and that of the asymmetric PO_2^-.

The four poly(glycoamidoamine)s affected the intensity and wavenumber shifts of these base vibrations to different extents (Figure 10). For example, intensity changes in both guanine stretches were most pronounced for **T4**, and the strongest pDNA binders (**G4** and **T4**) showed significant frequency shifts from 1492 to 1487 cm^{-1} and from 1491 to 1482 cm^{-1}, respectively. Intensity effects for the asymmetric phosphate band were greatest for **G4** and **T4** interactions with pDNA; however, minor changes in this frequency were observed for all of the polymers. The hyperchromicity of the **G4** and **T4** polyplexes at N/P = 2.5 for all wavenumbers (Figure 10 and Supporting Information) is reproducible and will be further investigated.

Discussion

The mechanism involved in polycation−DNA binding and compaction is not well understood, and such fundamental studies are important in many areas of research. Consequently, we have performed a thorough study on polyplexes formed with poly(glycoamidoamine)s and pDNA to elucidate the role of the hydroxyl number and stereochemistry in the pDNA binding affinity. All of the obtained results suggest that these polymers interact with pDNA through a dual mechanism of electrostatics (long-range, nonspecific, charge−charge interactions) and hydrogen bonding (short-range, directional, dipole−dipole interactions) and that the extent of the latter is dependent upon the carbohydrate in the repeat unit. It also appears that at least some binding is occurring through the base pairs of the polynucleotide.

The polyplexes were formed at various N/P ratios representing progressing states of complexation and were examined via dynamic light scattering and zeta potential. As polymer is titrated into the pDNA solution, the particle size remained steady around 200 nm until charge neutrality was reached, and then large-scale aggregation occurred (Figures 2 and 3). It was generally observed that the stronger the pDNA interaction, the less polymer amount that was needed to induce aggregation of the resultant polyplexes. As a side note, the positive surface charge of these polyplexes is thought to be important for cellular uptake mechanisms, which may occur through negatively charged proteoglycans extending from the membrane.

Determining the point of aggregation onset enabled simplification of the ITC curves, the fit of the data (Figure 4) to a simple algorithm, and the calculation of pDNA binding energetics. ITC injection points containing heats from contributions other than binding must be removed from the isotherm before attempting nonlinear least-squares regression analysis because the fitting models are based on an equilibrium saturation phenomenon. Once this was accomplished, the two-site model was able to fit the data well.

As highlighted in Figure 11, because of the dual nature of the copolymer (i.e., the existence of both carbohydrate and oligoamine units), many different interactions, such as charge−charge, hydrogen bonding, and hydrophobics, could contribute to the binding. The secondary amines that are protonated at pH 7.4 have an electrostatic attraction to the phosphate groups in the DNA backbone; however, the more unanticipated result was that

(38) Bloomfield, V. A.; Crothers, D. M.; Tinoco, I. *Physical Chemistry of Nucleic Acids*; Harper & Row: New York, 1974; pp 132−147.

(39) (a) Gray, D. M.; Ratliff, R. L.; Vaughan, M. R. In *Spectroscopic Methods for Analysis of DNA*; Methods in Enzymology; Academic Press: New York, 1992; Vol. 211, pp 389−397. (b) Rodger, A.; Norden, B. *Circular Dichroism and Linear Dichroism*; Oxford University Press: Oxford, U.K., 1997; pp 1−131.

(40) Tunis-Schneider, M. J. B.; Maestre, M. F. *J. Mol. Biol.* **1970**, *52*, 521−541.

(41) Marvin, D. A.; Spencer, M.; Wilkins, M. H. F.; Hamilton, L. D. *J. Mol. Biol.* **1961**, *3*, 547−565.

(42) (a) Taillandier, E.; Liquier, J. In *Spectroscopic Methods for Analysis of DNA*; Methods in Enzymology; Academic Press: New York, 1992; Vol. 211, 307−335. (b) Taillandier, E.; Liquier, J.; Taboury, J. A. *Adv. Infrared Raman Spectrosc.* **1985**, *12*, 65−113. (c) Arakawa, H.; Ahmed, R.; Naoui, M.; Tajmir-Riahi, H. A. *J. Biol. Chem.* **2000**, *275*, 10150−10153. (d) Taillandier, E.; Taboury, J. A.; Adam, S.; Liquier, J. *Biochemistry* **1984**, *23*, 5703−5706.

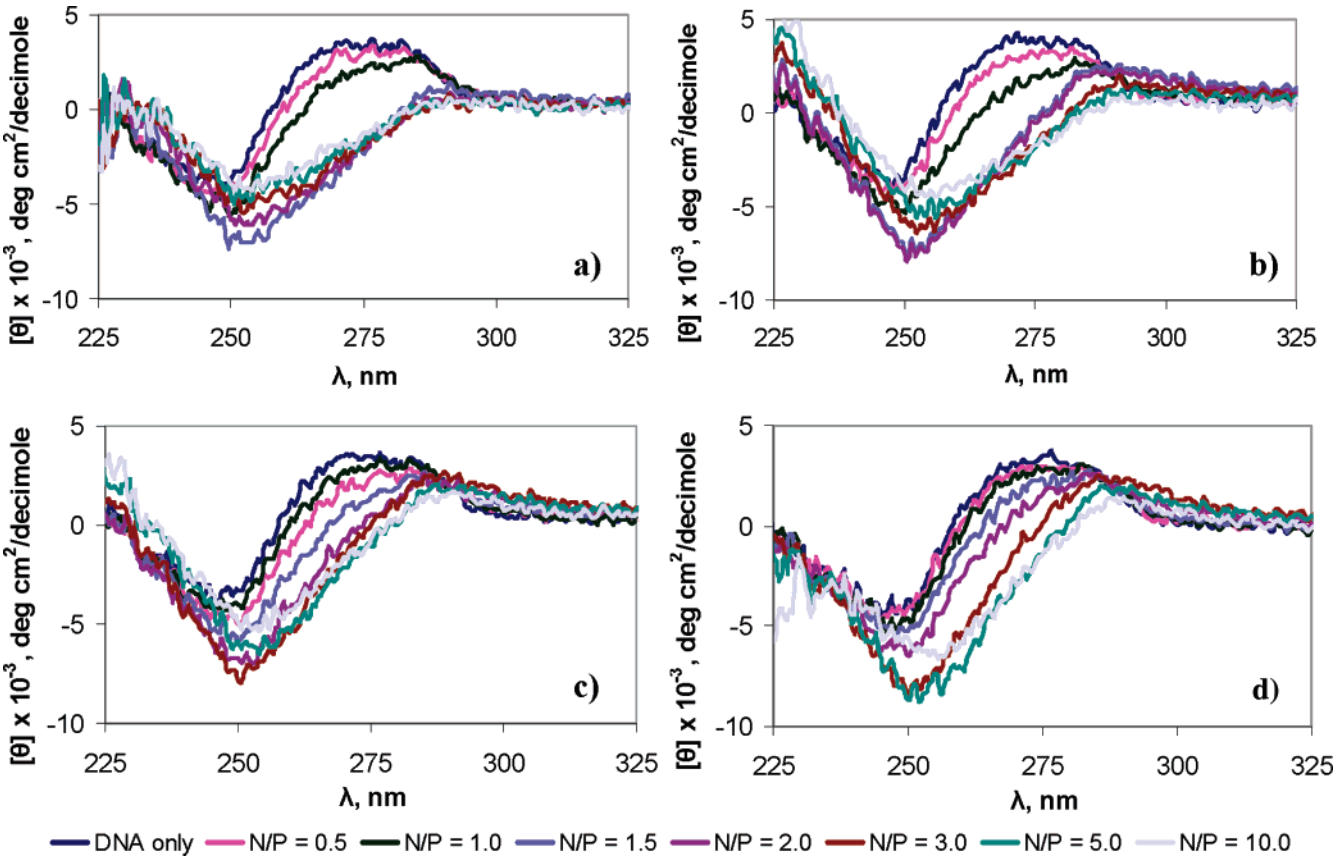

Figure 8. Circular dichroism (CD) spectra of 0.31 mM pDNA in 10 mM Tris (pH 7.4) buffer titrated with 5.5 mM (a) **G4**, (b) **T4**, (c) **D4**, or (d) **M4** at N/P = 0 (DNA only) (navy-blue line), 0.5 (black line), 1.0 (bright pink line), 1.5 (medium-blue line), 2.0 (darker-maroon line), 3.0 (lighter-maroon line), 5.0 (green line), and 10.0. (light-blue line).

the amines and/or the carbohydrate hydroxyl groups appear to be involved in another type of interaction with pDNA. This nonelectrostatic contribution to PGAA−pDNA complexation manifested itself in the isotherm as a second phase of binding.

We have shown through the calculation of octanol−water partition coefficients (data in Supporting Information) that the four PGAAs have comparable (and negligible) hydrophobicity. The entropic component to the binding free energy, $\Delta S°$, was also revealed through ITC to be 20−30 cal/mol K for all four of the polymers, indicating that hydrophobic interactions (which are entropically driven at 25 °C) are equal among the series. This information is very important to eliminating the hydrophobic effect as a source of the significantly different binding affinities of these polymers. This evidence, combined with the fact that various hydrogen bond donors and acceptors exist on the DNA molecule, such as phosphodiesters, amines, and carbonyl groups, renders hydrogen bonding a valid candidate for this other interaction (Figure 11). Many studies have shown that nucleic acids can interact strongly and specifically with polysaccharides[43] and aminoglycoside antibiotics[44] through the formation of hydrogen bonds (in particular, H bonding from the carbohydrate hydroxyl groups to the base pairs). The similarity of these structures to our poly(glycoamidoamine)s also influenced the assignment of this other force to hydrogen bonding. Hydrogen bonding was first suspected to play a role in the PGAA−pDNA binding affinity in a series of cell transfection and polyanion competition studies completed earlier in our laboratory.[8] These experiments generally revealed that the higher the polymer−pDNA binding affinity (qualitatively determined through heparin displacement assays), the higher the pDNA delivery efficiency. The directionality of hydrogen bond formation between the hydroxyl groups and the DNA molecule likely causes the carbohydrate stereoisomers in the repeat unit of these polymers to have such a dramatic effect on their binding efficiency.

The two-site binding theory assumes that the sites are independent and that binding is nonspecific. Nonspecific interactions are a reasonable assumption in this case because electrostatics, which are thought to drive polycation−DNA association, are independent of base pair sequence. However, the selection of a binding model based on two independent sites may be inadequate. Hydrogen bonding between the carbohydrate hydroxyl groups and pDNA is most likely enabled by long-range Coulombic attraction, which could be more accurately reflected in a model accounting for cooperativity within each phase. Whether cooperativity exists between sites 1 and 2 remains unclear. Because of the complexity of accounting for the many coupled interactions existing between these macromolecules, we have currently chosen to rely on the parameters given by the excellent fit of our data to the two-site independent model.

A valid hypothesis for the origin of isotherm shape is that the three phases observed in the polycation−pDNA association are attributable to a combination of electrostatics, hydrogen bonding, and condensation/aggregation of the polyplexes. It is important to note that although the longer-range charge−charge attraction is probably necessary to initiate binding, once in the proper vicinity for hydrogen bonding to occur, the two interactions are likely

(43) (a) Sakurai, K.; Shinkai, S. *J. Am. Chem. Soc*. **2000**, *122*, 4520−4521. (b) Sakurai, K.; Mizu, M.; Shinkai, S. *Biomacromolecules* **2001**, *2*, 641−650.

(44) (a) Fourmy, D.; Recht, M. I.; Blanchard, S. C.; Puglisi, J. D. *Science* **1996**, *274*, 1367−1371. (b) Sucheck, S. J.; Wong, C.-H. *Curr. Opin. Chem. Biol*. **2000**, *4*, 678−686.

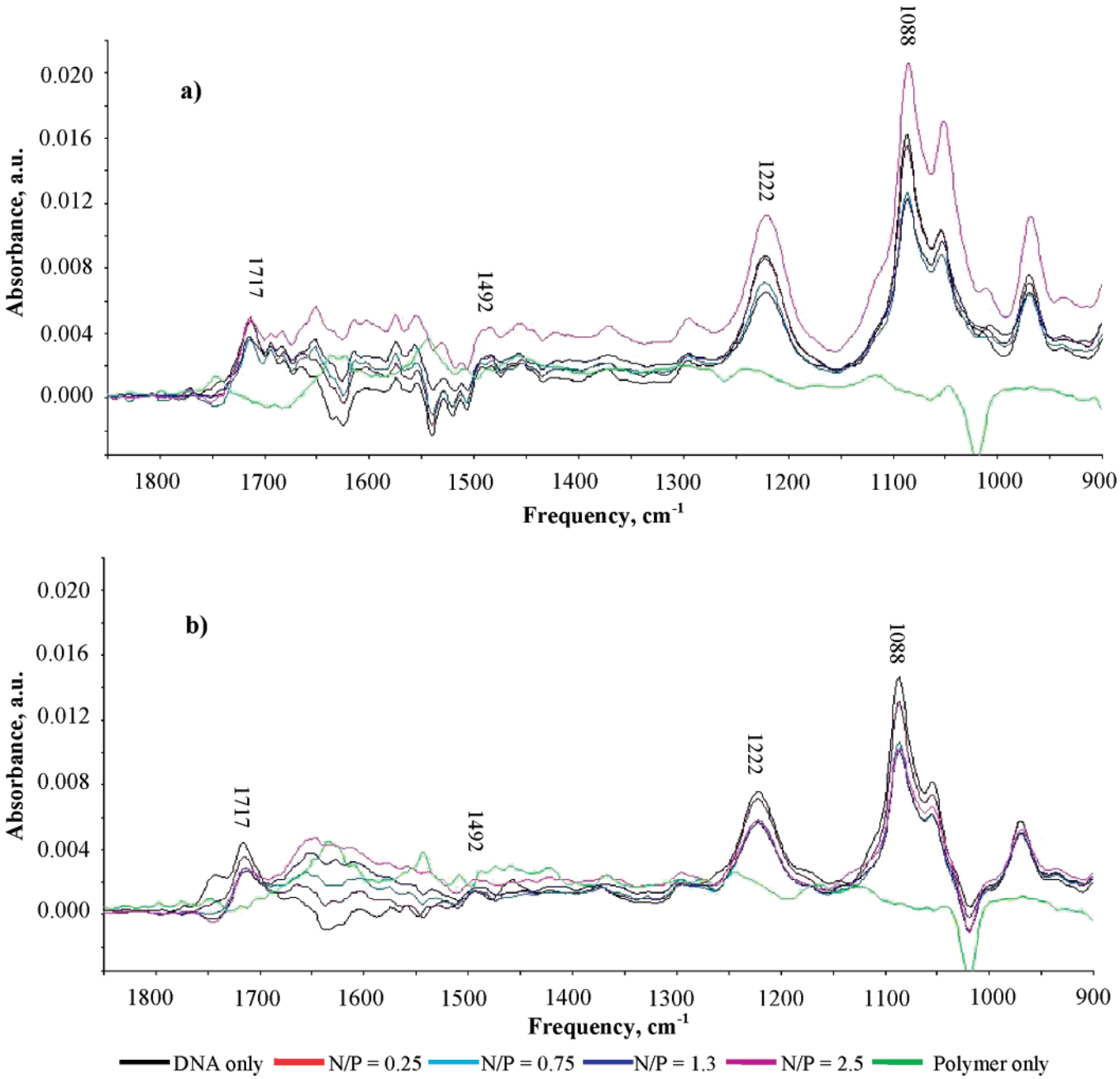

Figure 9. FTIR spectra of (a) **G4** and (b) **D4** polyplexes formed at N/P = 0 (DNA only) (black line), 0.25 (red line), 0.75 (turquoise-blue line), 1.3 (navy-blue line), and 2.5 (maroon line) in 10 mM Tris buffer (pH 7.4) at 25 °C. Polymer-only spectra are shown overlapping (green line).

in equilibrium. Thus, the assignment of each phase to a specific type of interaction is not possible; however, it can be assumed that each phase has a predominant contribution. Because Coulombic attraction is a long-range force and hydrogen bonding requires close proximity, we have assigned sites 1 and 2 to be primarily electrostatic and hydrogen bonding in nature, respectively.

We expected that the electrostatic contribution would be similar among **G4**, **D4**, **M4**, and **T4**, which correlated well (with the exception of **D4**) with the thermodynamic data from site 1. Assuming that the second slope in the isotherm, corresponding to site 2, incorporates a greater hydrogen-bonding contribution than the first explains the more marked difference among the values of K_2 than among the values of K_1 for the four poly(glycoamidoamine)s. As shown in Table 3 where the binding order is **G4** > **T4** > **D4** > **M4**, the stereochemistry of the hydroxyl groups in the carbohydrate does affect the binding strength, leading to the conclusion that these groups *are* involved in hydrogen bonding to pDNA. The higher ΔS_2 values for **G4** and **T4** likely represent the release of more solvent molecules due to the additional hydrogen-bonding interaction that these two PGAAs have with pDNA.

To examine our hypothesis that nonelectrostatic interactions between the polymer and the pDNA base pairs play a significant role in the observed binding affinity, circular dichroism and FTIR spectral changes were measured at various points of complex formation (Figures 8 and 9). The shapes of the CD curves are determined by the $\pi \rightarrow \pi^*$ electronic transition of the purine and pyrimidine bases.[38] As the interaction between the bases is altered, for instance, as a result of DNA compaction or direct hydrogen bonding by a ligand, these transitions are affected, which can be revealed as a shift in the spectrum or a loss of ellipticity.

Figure 8 demonstrates the different magnitudes of the spectral shift and the rotational strength changes instigated by poly-

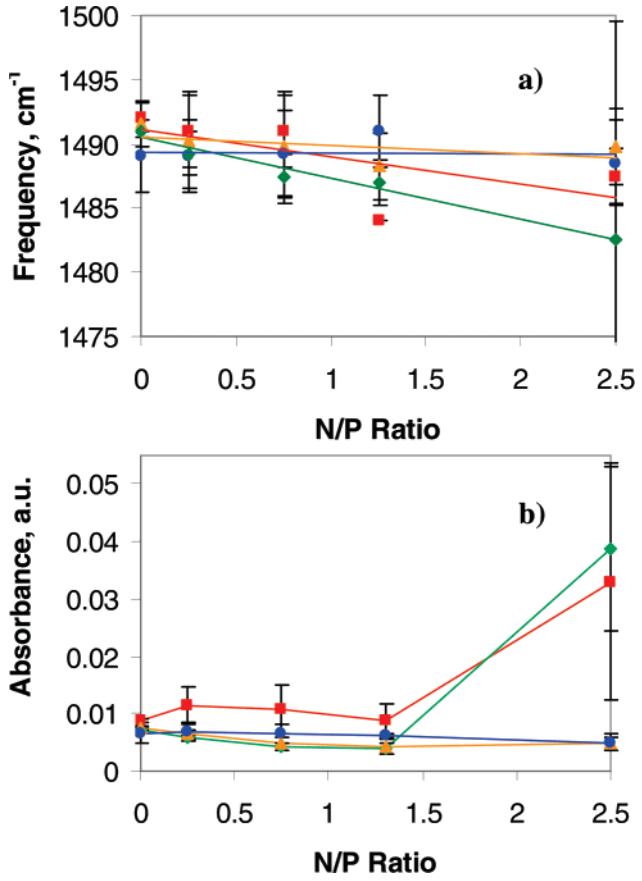

Figure 10. (a) Frequency shifts of the guanine 1492 cm^{-1} vibrational mode and (b) intensity changes for the phosphate 1222 cm^{-1} asymmetric stretch for pDNA upon complexation with (■) **G4**, (◆) **T4**, (▲) **D4**, and (●) **M4** at increasing N/P ratio.

(glycoamidoamine) binding. The CD spectra for **G4** and **T4** complexation with pDNA suggest a B → C change. However, it must be noted that the polycation-induced DNA secondary structure change from B → C is under scrutiny in the literature owing to X-ray diffraction and IR evidence that the C form retains characteristics still within the confines of B-DNA.[33,45] Regardless of whether the series of spectra for the tightest binders indicates a B → C conformational change, there is a significant effect on the separation of the base pairs, the base−helix incline angle, and the pitch of the helix, evidencing a strong interaction between our polymers and the pDNA base pairs. Such drastic deformation of the rotational bands cannot be explained by simple compaction of the double helix. We know, on the basis of particle size measurements reported previously,[8,9] that all of the poly(glycoamidoamine)s (and PEI) compact pDNA, but the CD spectra for **D4**, **M4**, and PEI[35] over various N/P ratios do not show the extent of changes witnessed with the **G4** and **T4** interactions. Thus, the different affinities of **G4**, **T4**, **D4**, and **M4** for pDNA (seen through the ITC and ethidium bromide assay data) are perhaps due to the easier formation of hydrogen bonds with the base pairs as a result of hydroxyl stereochemistry and their alignment with the DNA base hydrogen-bond acceptors.

In an attempt to ascertain which DNA sites are involved in interactions with each PGAA, FTIR spectra of each polyplex at

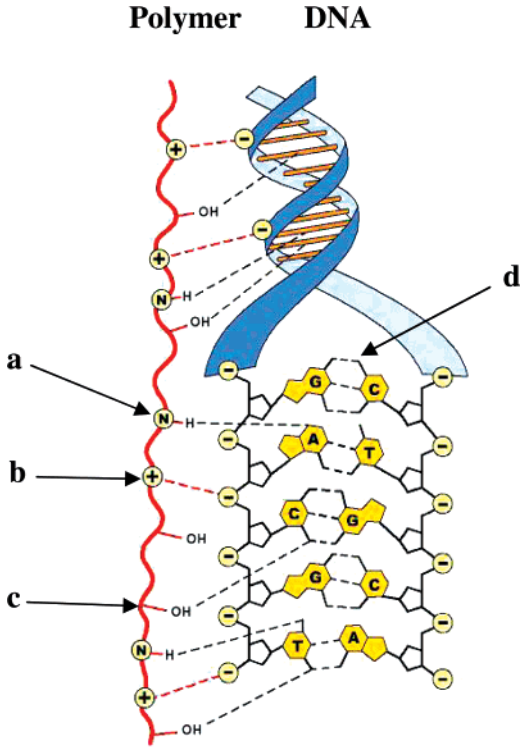

Figure 11. Illustration of pDNA−PGAA binding demonstrating both electrostatics and possible sites of hydrogen bond formation. (a) Hydrogen bond between the polymer amine and base, (b) electrostatic interaction between the protonated amine and phosphate group, (c) hydrogen bond between the carbohydrate hydroxyl group and base, and (d) hydrogen bonds between base pairs.

N/P = 0−2.5 were obtained. Because of overlap from both inevitable water vapor and the amide stretch of the glycopolymers, the thymine (1663 cm^{-1}) and adenine (1609 cm^{-1}) vibrations could not be analyzed (Figure 9 and Supporting Information). The phosphate symmetric (1088 cm^{-1}) and asymmetric (1222 cm^{-1}) bands showed minor frequency shifts upon PGAA binding; however, there were significant intensity changes here, especially for **G4** and **T4** (Figure 10). Intensity effects have been attributed not only to direct binding but also to helix stabilization; therefore, these results indicate an alteration of base stacking and base pairing upon interaction with the poly(glycoamidoamine)s,[42,46] which is consistent with the circular dichroism data. This could be a consequence of either polycation-induced DNA condensation or direct interactions. In the case of the guanine carbonyl (1717 cm^{-1}) and imidazole nitrogen (1492 cm^{-1}) vibrations, more modest intensity variations are shown. Although no significant frequency shift occurred at 1717 cm^{-1} for any of the four polymers (Figure 9), **G4** and **T4** binding did induce a shift of the imidazole nitrogen vibration to lower wavenumbers, especially at higher N/P ratios. This suggests that the stronger pDNA binders, **G4** and **T4**, may have direct interactions with the imidazole nitrogen, whereas all other PGAA−base associations are likely indirect through localized water molecules.[46]

The deconvolution of both **G4**− and **D4**−pDNA binding free energies into electrostatic and nonelectrostatic contributions (Table 5) further supports the existence of electrostatic and hydrogen-bonding coupling in all stages of the polycation−pDNA association. When NaCl was added to the buffer solution for the

(45) (a) Zimmerman, S. B.; Pheiffer, B. H. *J. Mol. Biol.* **1980**, *142*, 315−330. (b) Hirsch-Lerner, D.; Barenholz, Y. *Biochim. Biophys. Acta* **1999**, *1461*, 47−57. (c) Choosakoonkriang, S.; Wiethoff, C. M.; Kueltzo, L. A.; Middaugh, C. R. In *Nonviral Vectors for Gene Therapy*; Findeis, M. A., Ed.; Methods in Molecular Medicine; Humana Press: Totowa, NJ, 2001; Vol. 65, pp 285−317. (d) Braun, C. S.; Jas, G. S.; Choosakoonkriang, S.; Koe, G. S.; Smith, J. G.; Middaugh, C. R. *Biophys. J.* **2003**, *84*, 1114−1123.

(46) (a) Ouameur, A. A.; Tajmir-Riahi, H. A. *J. Biol. Chem.* **2004**, *279*, 42041−42054. (b) Benevides, J. M.; Stow, P. L.; Ilag, L. L.; Incardona, N. L.; Thomas, G. J. *Biochemistry* **1991**, *30*, 4855−4863. (c) Ruiz-Chica, J.; Medina, M. A.; Sanchez-Jimenez, F.; Ramirez, F. J. *Biochem. Biophys. Res. Commun.* **2001**, *285*, 437−446.

ITC experiments, $\Delta G°_{es}$ revealed that both sites 1 and 2 have similar degrees of electrostatic interaction for **D4**. However, in the case of **G4**, $\Delta G°_{es}$ decreased in magnitude, and the nonelectrostatic component to the binding increased from site 1 to site 2. This supports our assignment of site 2 as the more hydrogen bonding-rich interaction and that it is enhanced in the **G4**−pDNA association probably because of the stereochemistry of galactarate hydroxyl groups and directional hydrogen bonding to the pDNA molecule. Also, as the concentration of monovalent ions in solution increased from 15 to 300 mM, the charge−charge association between both **G4** and **D4** and pDNA decreases significantly (the expected result of shielding), as shown by the decrease in magnitude of $\Delta G°_{es}$. The magnitude of the $\Delta G°_{ns}$ free-energy contribution displays the fact that hydrogen bonding is the major binding mode at sites 1 and 2 for these two polymers and that the presence of charges on a ligand does not necessitate that electrostatics makes a dominant contribution to binding. Such a conclusion is in contrast to the accepted mechanism of charge−charge polycation association with DNA, although it mimics the hydrogen bonding seen with other carbohydrate-based drugs[44] and polymers.[43]

The ability of PGAAs containing different carbohydrate structures to complex pDNA was indicated by their ITC binding constants (**G4** > **T4** > **D4** > **M4**, as shown in Table 3). The results obtained from EB exclusion (**T4** ≥ **G4** > **D4** > **M4**) are an indirect indication of pDNA affinity, as was the case for the heparin-displacement assay conducted previously by our group that showed a similar pDNA binding strength order.[8] Qualitative techniques such as these, which are commonly used in the field of nonviral delivery vectors, have many drawbacks. For instance, IC_{50} values obtained via EB exclusion are indicative of the ability of a competitor to displace ethidium bromide from its intercalated location between the nitrogenous bases of DNA. This is usually thought to be due to the compaction event, which may be directly related to binding strength (compaction is caused by pDNA charge neutralization). Different mechanisms of binding (i.e., the extent of base pair interaction) could greatly affect the compaction phenomenon and, hence, ethidium exclusion results. Also, the heparin competition assay relies on the ability of a polyanion competitor to displace pDNA in the polymer−pDNA complex. Different polymers can have varying affinities for heparin, which would certainly skew the results of polycation−DNA interaction strength. These limitations are demonstrated by the inability of the EB assay to distinguish between the significant (1 order of magnitude) enhancement of binding between **G4** and **T4** and pDNA (Figure 5), revealed through ITC experiments (Table 3). The IC_{50} values determined via EB assay did, however, reflect the base pair spacing and tilt changes upon binding that we witnessed by CD and FTIR. Enhanced interaction of **G4** and **T4** with the nucleotide bases of pDNA could reasonably affect the exclusion of the ethidium molecule from its intercalated position.

During the association at physiological pH, 0.07−0.15 moles of protons are taken up per mole of secondary amine according to the ITC study of PGAA−pDNA binding in the presence of varying buffers (Figure 6). The reasonable assumption that the binding-linked protonation of all four PGAAs would be comparable because of their identical amine moieties was challenged by the fact that the difference in binding strength affects a different pK_a shift of the ionizable groups. Thus, the order of pDNA affinity is reflected in the moles of protons per mole of secondary amine taken up by the polymer upon binding [**G4** (0.15) > **T4** (0.13) > **D4** (0.11) > **M4** (0.072)].

This protonation information is very valuable in understanding the mechanism of binding of these new polymeric gene delivery vehicles as well as their buffering capacity, which may or may not aid in polyplex endosomal release by the "proton sponge" hypothesis,[3b,47] At physiological pH, these structures have been shown to possess roughly 20% protonation.[48] Therefore, despite this binding-linked protonation, approximately 65% of the polymer secondary amines remain unprotonated and can participate in hydrogen bonding to DNA, along with the hydroxyl groups in the carbohydrate unit. This also means that 65% of the amines are available for buffering in the endosomes. The importance of buffering capacity for gene transfection is currently under scrutiny; however, a binding-linked protonation study such as the one performed here is crucial to discovering the true buffering capacity after polyplex formation. As shown by these results, binding mechanisms and strength can influence proton uptake and, hence, the ability of these vectors to facilitate endosomal escape.

Incorporation of carbohydrate moieties into the polymer repeat unit was originally performed to reduce cytotoxicity; however, according to this detailed mechanism analysis, an additional role is clearly one of enhanced binding. As previously shown by our group, approximately 20% of the secondary amines in these polymers are protonated at physiological pH.[48] The large association constants obtained for **G4** and **T4**, on the order of more densely protonated polyamines, seem to imply additional sources of attraction. The stereochemistry, more than the number, of hydroxyls in each carbohydrate unit obviously plays a determining role in the strength of this interaction. Interestingly, **T4**, possessing only two hydroxyl groups, does not hinder its ability to bind pDNA, as evidenced by its K_2 association constant of 1.96×10^6 M^{-1} (1 and 2 orders of magnitude greater than those of **D4** and **M4**, respectively, which each contain four hydroxyls). The orientation of the H-bond donor groups of the carbohydrates within **G4** and **T4** repeat units must be conducive to the strict directionality of hydrogen bond formation, thus aiding stronger pDNA complexation.

It is important to note that polymer−polymer interactions have not been considered in this analysis. The possibility certainly exists that the carbohydrate hydroxyl groups and/or backbone secondary amines are hydrogen bonding with each other and that one carbohydrate may have enhanced interaction over another because of stereochemistry. Galactaric acid has been shown via crystal structure determination to form strong intermolecular hydrogen bonds.[49] This characteristic is reflected in its low water solubility, a property that D-mannaric acid and D-glucaric acid do not possess. Whether polymer−polymer association plays a role in the PGAA−pDNA binding mechanism and, if so, how this affects the formation of polyplexes are currently being investigated.

Conclusions

The transfection of therapeutic genes into cells is a complex process consisting of DNA packaging, cell targeting, avoiding degradation, cellular uptake, and intracellular trafficking and release of the material. Vector−DNA complexation is a crucial first step that determines not only polyplex physical properties (size, charge, morphology, and stability) but also DNA protection, competitive displacement, and eventual DNA release capabilities. Previous work has implied that the strength of interaction between PGAA nucleic acid delivery vectors and DNA is dependent upon

(47) (a) Behr, J.-P. *Chimia* **1997**, *51*, 34−36. (b) Kulkarni, R. P.; Mishra, S.; Fraser, S. E.; Davis, M. E. *Bioconjugate Chem.* **2005**, *16*, 986−994. (c) Godbey, W. T.; Barry, M. A.; Saggau, P.; Wu, K. K.; Mikos, A. G. *J. Biomed. Mater. Res.* **2000**, *51*, 321−328.
(48) Liu, Y.; Reineke, T. M. *Bioconjugate Chem.* **2007**, *18*, 19−30.
(49) Jeffrey, G. A.; Wood, R. A. *Carbohydr. Res.* **1982**, *108*, 205−211.

both charge density and hydroxyl stereochemistry.[5,7−9] Herein, we have dissected the fundamental driving forces of the specific interactions between pDNA and these PGAA vehicles. Although binding strength is only one aspect of the transfection pathway, such mechanistic studies are important to the field of biomaterial design to understand the physical and chemical parameters that enhance the efficacy of polyplex-mediated gene delivery.

This study suggests that, in addition to lowering toxicity, the incorporation of carbohydrate groups into polycations can greatly enhance their pDNA interaction. Although the association of PGAAs with pDNA was found to be entropically driven, which is typical for materials incorporating electrostatic binding, the differences in the K_2 values obtained via ITC for polymers varying only in hydroxyl number and stereochemistry hint that hydrogen bonding interactions play an important role in PGAA−pDNA binding affinity. Ethidium bromide exclusion assay results and the deconvolution of binding free energy into its electrostatic contribution also support this finding. In fact, the free-energy components of the PGAA−pDNA association imply that hydrogen bonding is the dominant force. Specific hydrogen bond formation with pDNA bases was suggested by the infrared vibrational shifts, base pair separation, and tilt angle increments upon addition of polymer to pDNA solution through circular dichroism measurements. All of these results support the hypothesis that the stereochemistry of hydroxyls in the carbohydrate monomer of the repeat unit determines the ability to form complex-enhancing hydrogen bonds to pDNA.

The determination of the pDNA binding mechanism of the poly(glycoamidoamine)s has many implications in understanding structure−property relationships of gene delivery vehicles. The binding-linked protonation results indicate that the polymers have less buffering capacity than previously suggested, and this information can contribute to determining the validity of the "proton sponge" hypothesis. The importance of hydrogen bond formation implies that base sequence-specific interactions may be involved, in which case strong DNA binders could be tailored to the therapeutic strand of interest. Incorporating strong hydrogen-bonding moieties into polymeric vectors could also eliminate the need for high charge density, which is thought to contribute to cytotoxicity. The rational design of future transfection agents depends on elucidating the complex mechanisms involved in their function both inside the cell and before the polyplex ever reaches the cell surface membrane.

Acknowledgment. We thank Professor Bjorn Lindman (Lund University) for helpful discussions on the driving forces behind DNA−polycation interactions, Amanda Ramey and Dr. Yemin Liu for synthesizing some of the polymers used in these studies, and Lisa Bartholomew for completing two of the ethidium bromide exclusion assays. We also thank Professor Bruce Ault for FTIR spectroscopy support and Apryll Stalcup (University of Cincinnati) for the use of her CD spectrometer. This work was supported by The National Science Foundation CAREER Award program (CHE-0449774). T.M.R. acknowledges support by the Alfred P. Sloan Research Fellowship program.

Supporting Information Available: Isothermal titration calorimetry (ITC) thermograms for **G4**, **D4**, and **M4**, FTIR spectra for **T4** and **M4** polyplexes, and experimental methods and results for octanol/water partitioning for all four PGAAs. This material is available free of charge via the Internet at http://pubs.acs.org.

LA7009995